



Research Article

Extraction and Analysis of Spatial Feature Data of Traditional Villages Based on the Unmanned Aerial Vehicle (UAV) Image

Zun Teng ¹, Chuntao Li ¹, Wenjing Zhao,¹ Zuxiang Wang,² Ruonan Li,¹ Lang Zhang,³ and Yuqing Song⁴

¹School of Forestry and Landscape Architecture, Anhui Agricultural University, Hefei 230036, China

²Chaohu City Garden Management Office, Chaohu 238000, China

³Shanghai Academy of Landscape Architecture Science and Planning, Shanghai 200232, China

⁴School of Foreign Studies, Anhui University, Hefei 230601, China

Correspondence should be addressed to Chuntao Li; lichuntao@ahau.edu.cn

Received 18 September 2022; Revised 20 November 2022; Accepted 30 November 2022; Published 26 December 2022

Academic Editor: Mahdi Abbasi

Copyright © 2022 Zun Teng et al. This is an open access article distributed under the Creative Commons Attribution License, which permits unrestricted use, distribution, and reproduction in any medium, provided the original work is properly cited.

In the process of the evolution of urban-rural spatial patterns, traditional village forms have been seriously eroded and destroyed, resulting in the gradual loss of garden feature elements and the blurring of spatial features. Facing these problems, accurate and efficient acquisition of relevant data becomes the key to traditional village conservation. We take the typical Huizhou Shuikou garden Tangmo village as an example and conduct a study on how to use UAV aerial images to extract spatial feature data. Firstly, the UAV was used to acquire aerial images of the study area through a predefined mission. Then, the image data are processed by using structure from motion (SfM) software to obtain digital surface model (DSM), digital orthophoto map (DOM), point cloud, and 3D model. Finally, the produced spatial data are applied to the spatial feature extraction analysis study. The results show the following: (1) the data produced by UAV aerial images have a horizontal accuracy of 0.034 m and a vertical accuracy of 0.039 m, which meet the requirements of traditional village spatial data collection. (2) The results of spatial feature elements and terrain feature extraction show that the 3D model and DSM can accurately extract and analyze the micro and macro spatial feature of traditional villages. (3) By using the cloth simulation filtering (CSF) to extract point clouds of buildings and streets, and after statistical analysis, we could quickly obtain their spatial features. Based on the spatial data obtained by using UAV, the study achieves the accurate collection of Tangmo DSM, DOM, 3D model, and spatial feature data and forms a method of data collection, processing and spatial feature extraction. The results of the study can provide a scientific basis for data collection on the spatial features of other cultural heritages and the conservation of traditional villages.

1. Introduction

As revitalized cultural heritages, traditional villages carry a large amount of human ecology, ethnic characteristics, architectural aesthetics, and social history and are a concentrated display of the regional traditional culture [1–3]. In 2018, the opinions of the “Central Committee of the Communist Party of China and the State Council on the Implementation of Rural Revitalization Strategy” issued by the Central Committee of the Communist Party of China and the State Council of China put forward clear requirements for the protection of traditional villages [4]. In recent

years, along with the rapid urbanization, traditional villages and residents’ production and lifestyle have been greatly affected [5]. Problems such as loss of cultural elements, building collapse, and encroachment of agricultural land have emerged, leading to changes in the original spatial features. Therefore, the collection of spatial data has become the key to the cultural heritage and spatial conservation of traditional villages.

At present, the research on traditional villages is mainly focused on two aspects: conservation and utilization [6]. Scholars have mostly discussed from the perspectives of spatial distribution features [7], environment [8], historical

and cultural factors, and tourism potential and development [9]. However, there are fewer studies on the spatial data collection of traditional villages. Some early studies obtained research data only by means of field surveys. For example, Xu and Chiou [10] used literature review and field research to obtain data on village landscape layout and geographic environment information. However, these data have some problems such as long acquisition time, lack of accuracy and subjectivity, and the manual mapping method are destructive to the cultural heritage of the investigated villages. With the development of information technology and spatial technology, 3S technology has been applied to the spatial data collection of traditional villages, e.g., Fu et al. [11] used 3S technology to investigate the data of selected traditional villages and establish a spatial database. Yang et al. [12] collected remote sensing images from different periods to process into multitemporal maps to obtain changed spatial data. Although these methods can acquire spatial data faster and avoid the destruction of cultural heritage, they are not the ideal way to collect spatial data of villages due to the influence of single form of data, image resolution, and cloud cover. In recent years, some scholars have used laser scanners for ground surveys to acquire 3D models and high-quality images, providing a method that is less subject to natural environmental images and easier to collect large amounts of data. For example, Lin et al. [13] used a laser scanner to scan and map cultural heritage buildings in Fenghuang Village, which were processed to obtain 3D models for analyzing the spatial features of the village architecture. Shao et al. [14] combined the data collected by ground laser scanning and structured the light scanner to obtain accurate and detailed 3D models. However, this type of equipment is expensive, requires more manual operation and time, and is not suitable for data collection at the village scale. Therefore, how to record the spatial features and landscape of traditional villages in the study and to achieve complete spatial data collection is an urgent problem to be solved. Along with the development of UAV technology, the data collection method based on oblique photography [15] provides a new option for the spatial data collection of traditional villages at small and medium scales.

As an emerging data collection platform, UAVs have the characteristics of small size [16], light weight [17], and flexibility [18, 19] and have been widely used in geographic mapping [20], disaster assessment [21, 22], and archaeological exploration [23, 24]. At present, UAVs are also widely used in the study of traditional villages, e.g., Sestras et al. [25] used drone image data and 3D reconstruction technology for ancient building restoration and tourism potential analysis. Hidayat and Muljo Sukojo [26] explored the accuracy of rotary-wing drones for producing large-scale base maps of villages. However, most of these studies focused on the application of collecting data on architectural space and planar space features, and there were relatively few studies on multiangle spatial data extraction for the whole village.

This paper introduces the application of UAV technology in spatial data collection and spatial feature extraction of traditional villages with Tangmo as the research object. DSM, DOM, point cloud, and 3D model data

produced by UAV images are used to extract spatial feature information from multiple angles, including village spatial feature elements, terrain, buildings, and street space. It provides a reference for the spatial information collection and digital conservation of traditional villages.

2. Study Area

The traditional village of Tangmo is a typical Huizhou Shuikou garden village, located in Qiankou Town, central Huizhou District, Huangshan City, Anhui Province, China (see Figure 1), only 10 km away from the ancient city of Huizhou. The village area is about 4 km², located in the hilly area. Influenced by the surrounding natural environment and geomantic thought, Shuikou Garden-Tangan Garden is built at the stream outlet. Shuikou is composed of spatial features such as Shadi pavilion, Xu's ancestral temple, and Yudai Bridge, forming a unique Shuikou garden space. However, with the development of tourism resources, the original spatial features of the village were changed [27]. As an important component of the Tangmo Shuikou garden space, the barge and bridge lines of Tangan River were recklessly changed. The original village space on both sides of the river has been encroached upon and the plant space has been created in a disorderly manner, especially the collapse and alteration of ancient buildings and other natural landscapes, resulting in the loss of the original unique architectural and street space features of the village. At the same time, due to the complex structure of the village, it is difficult to collect data in time, resulting in the lack of data to record and describe spatial features [28].

Therefore, there is an urgent need for spatial data collection and extraction methods that are near real-time and accurate. In this study, we selected the characteristic elements of the Shuikou garden space and the spatial extent of both sides of the Tangan River as the research objects.

3. Method

This study consists of four basic steps. The first step is aerial imagery and GNSS data collection of the study area. The second step is the processing of the aerial imagery acquired in flight using SfM software, which is used to generate photogrammetric products. The image processing steps include image alignment, sparse and dense point cloud generation, DSM, DOM, and 3D model production. The third step is spatial feature data extraction; using the produced 3D models, point clouds, and DSM spatial data, the spatial features of Tangmo villages are extracted from spatial elements, architectural street space, and terrain perspectives, respectively. The last step is the applied research, using the directly generated photogrammetry products and the extracted spatial feature data to build a spatial database to provide data support for the restoration and renewal of traditional villages (see Figure 2).

3.1. Flight Mission and Data Acquisition. In this study, the UAV DJI Mavic Zoom (see Table 1) was selected as the main instrument for image acquisition. This UAV is easy to

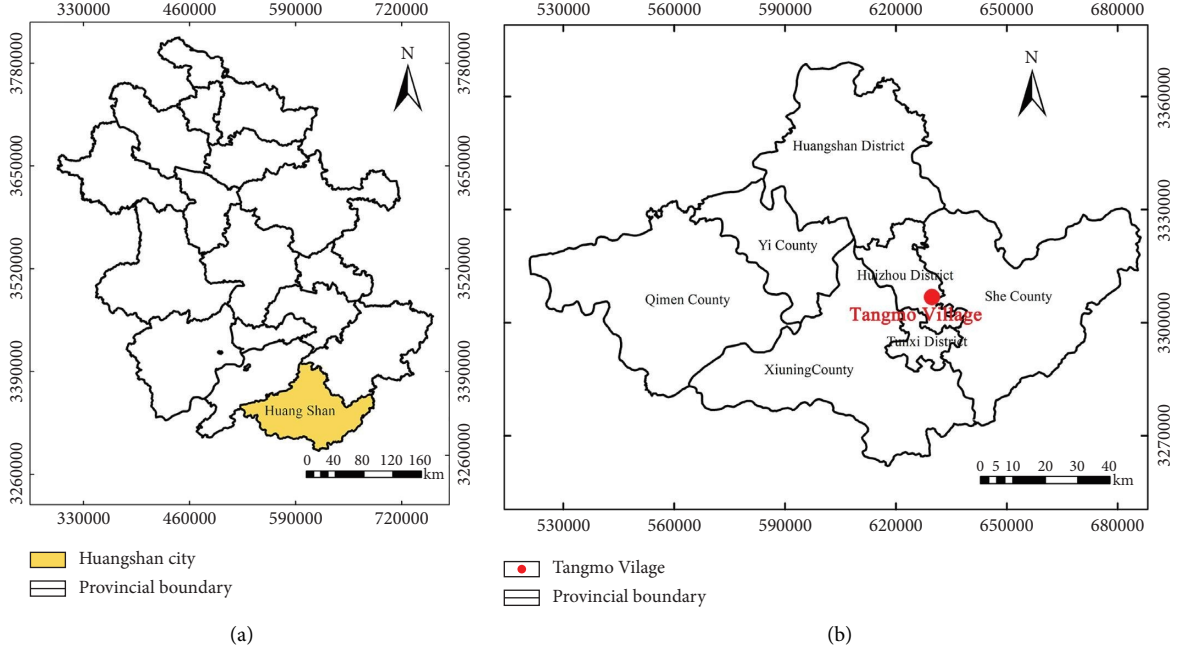


FIGURE 1: The geographic location of the study area. (a) Huangshan city. (b) Tangmo village.

operate and has built-in instruments such as GPS, optical obstacle avoidance lens, and compass, enabling the operator to monitor the vehicle's position, flight attitude, altitude, and speed in real time [29]. The active stabilization camera gimbal is capable of ensuring clear camera images despite tilting caused by the aircraft vibration and wind.

In the route planning of the flight plan. To meet the requirements of spatial information extraction and analysis of Tangmo villages, the ground resolution $G = 30$ mm is set. The flight altitude is calculated as 55 m according to the UAV camera specifications as follows:

$$H = \frac{P_w G f}{S_w}, \quad (1)$$

where P_w is the number of pixels on the long side of the camera, G is the ground resolution, f is the summed focal length, and S_w is the sensor width.

In order to avoid problems such as blurred images and photo overlap in the shooting, the flight speed, camera parameters, and the settings must also meet the corresponding requirements in the shooting [30]. The course overlap rate and side overlap rate were both set to 85%. The flight speed was 6.8 m/s, calculated from the camera settings, course overlap rate settings as follows:

$$V = \frac{HS_h(1 - O_h)}{fT_s}, \quad (2)$$

where S_h is the sensor height, O_h is the course overlap rate, and T_s is the exposure time interval.

DJI Pilot was selected as the flight control software for the mission, which is mainly for the use of single lens multirotor UAV and to meet the needs of single lens for oblique photography. The flight route was "S" shaped to cover the whole study area, with 5 flight routes. One of the

routes was a vertical photography route with a camera angle of 0 degrees. The remaining four routes were adjusted to a camera angle of 60 degrees to obtain the required images for oblique photography. The mission was carried out in two passes over Tangmo Village. The first mission was conducted with vertical photography, with 2 flights and 2,362 images. The second mission was conducted with oblique photography, with 4 flights, 4 routes completed, and 4023 images obtained.

In order to precisely locate the plane and elevation coordinates of ground control points, the Trimble R10 global navigation satellite system in the GPS-RTK mode was selected for this study [31]. The horizontal accuracy of the ground control points (GCPs) center coordinates measured by this instrument is 0.013 m–0.033 m, and the vertical accuracy is 0.030 m–0.055 m. To ensure that this accuracy range is reached, online RTK calibration provided by the BeiDou satellite-based system, the FindAUTO location positioning system is used. In addition, the GCPs should be evenly distributed in the study area and ensure that the surrounding area is free of obstructions and the point markings can be clearly identified.

3.2. Data Processing

3.2.1. The Output of Results. To obtain spatial data such as Tangmo DSM and 3D models. This study processed all suitable images in a complete and continuous workflow by using Context Capture software. The workflow includes importing image data, entering CMOS size, focal length and photo pixel information of the UAV camera, determining the location of control point coordinates in matching photos, aerial triangulation, and obtaining sparse and dense point clouds. Finally, the dense point cloud is used to

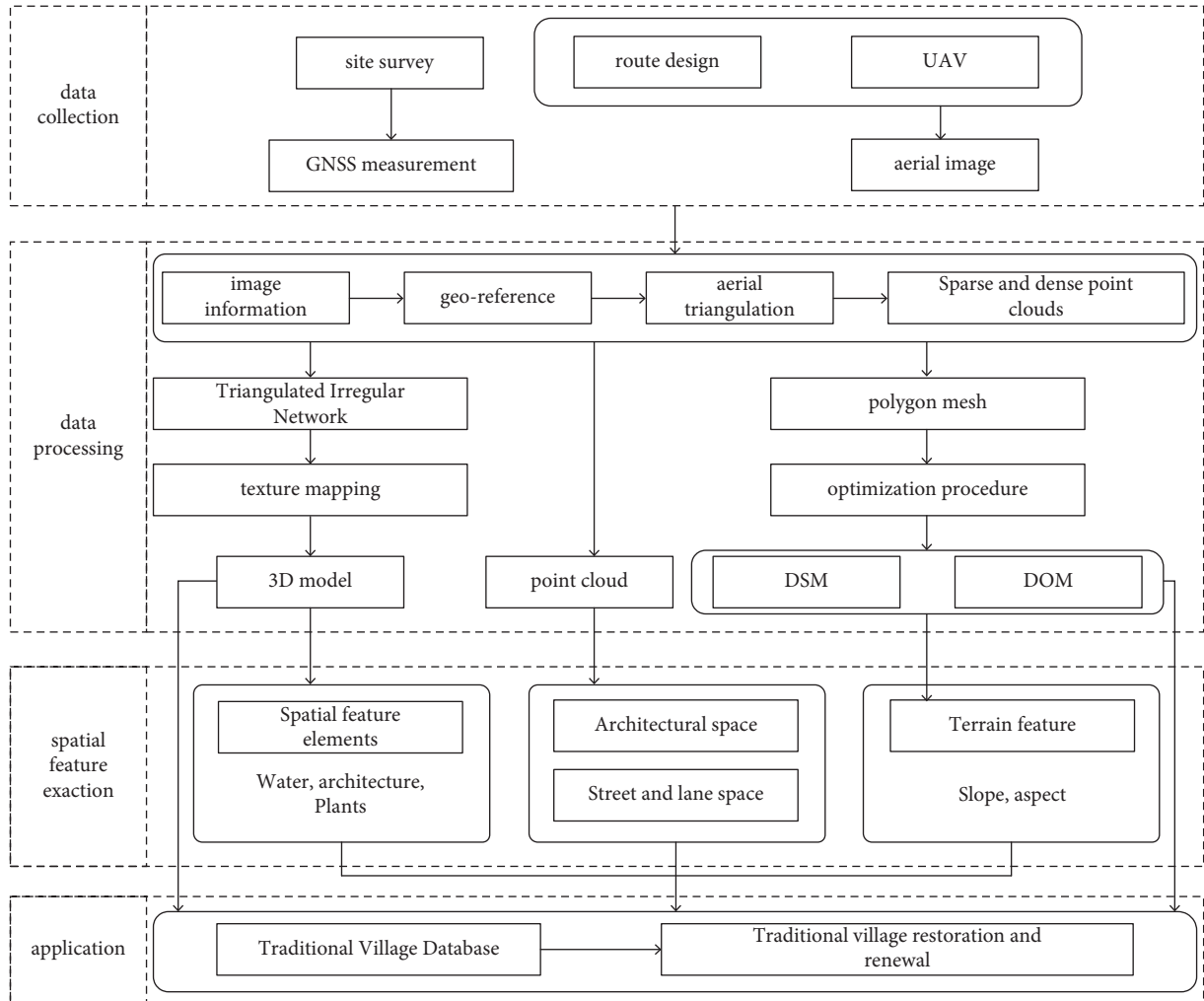


FIGURE 2: The methodological flowchart.

TABLE 1: Key parameters of the UAV.

UAV specifications	UAV parameters	Camera specifications	Camera parameters
Diagonal wheelbase	354 mm	Camera model	FC2204
Maximum take-off weight	905 kg	Image sensor	1/2.3 inch CMOS, effective pixel 12 million
Maximum altitude	500 m	Equivalent focal length	24–48 mm
GNSS	GPS + GLONASS	Camera angle	77°
Hovering accuracy	Vertical: ± 0.5 m, horizontal: ± 1.5 m	Lens iris	f/2.8 –f/3.8
Battery power	3850 mAh	Size of image	4000 \times 3000
Hovering time	29 min	Color pattern	Dlog-M (10 bit), HDR video (HLG 10 bit)

construct triangulated Irregular network and map the image texture in it to obtain 3D model. Based on the aerial triangulation results and dense point clouds, the complete DSM and DOM data are generated through the polygon mesh creation and automated processing.

3.2.2. Error Estimation. A total of 35 GCPs uniformly distributed over the study area were used as ground references during the geo-alignment process (see Figure 3). To check the accuracy and precision of the production results, the coordinates of the control points were measured in the

3D model using Acute3D Viewer software. The deviation values were calculated based on the northward, eastward, and elevation of the coordinate system. Among the 35 measured GCPs, 25 of them with more uniform distribution and distinctive features were selected as control points in the geographic alignment, and the remaining 10 were used as check points (CPs). See Tables S1 and S2 in the supplementary material for geographic coordinate values. The calculation results show that the RMSE is 0.034 m horizontally and 0.039 m vertically, which meets the accuracy requirements for the spatial feature extraction analysis study of traditional villages (see Figures 4 and 5).

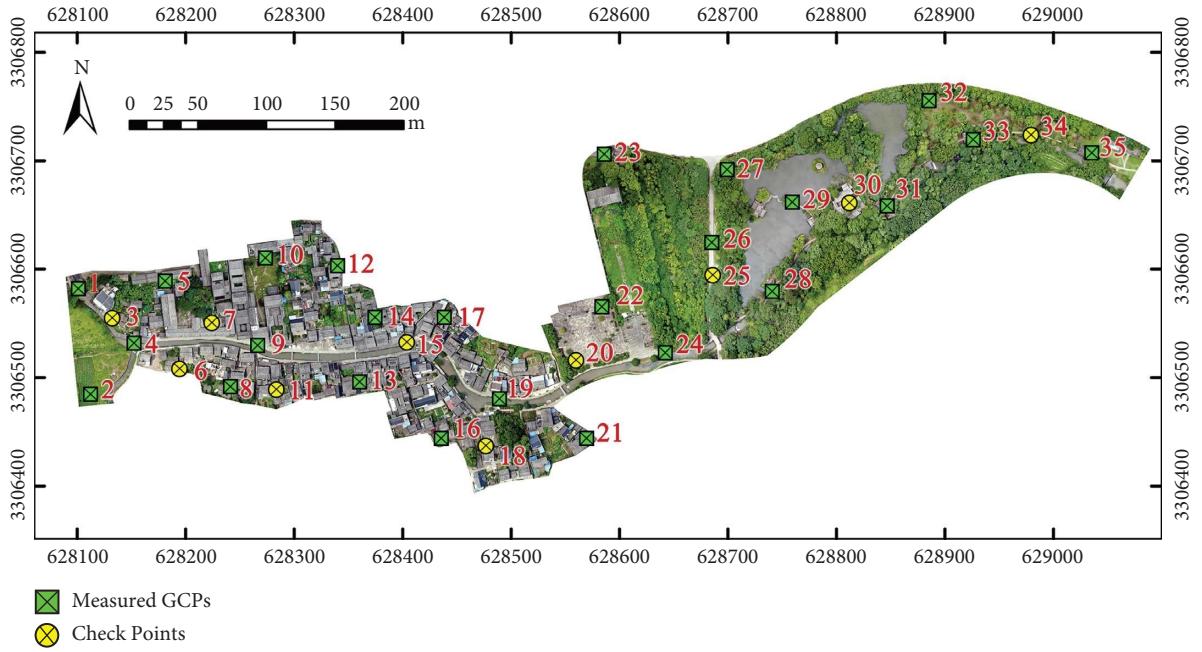


FIGURE 3: GCPs and CPs distribution map.

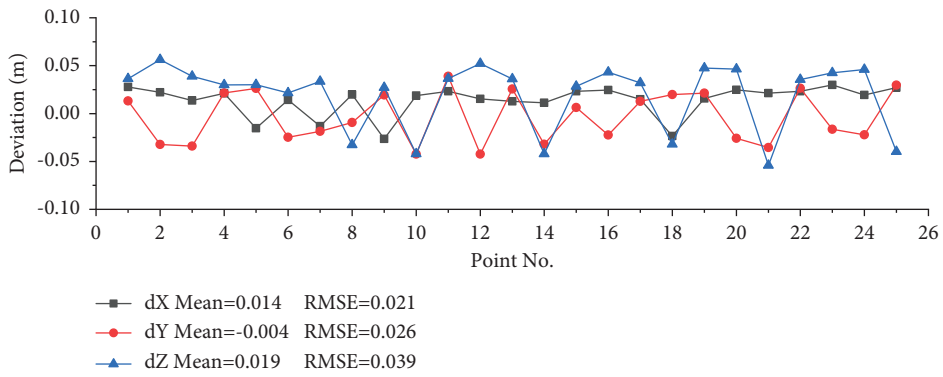


FIGURE 4: GCPs deviation figure.

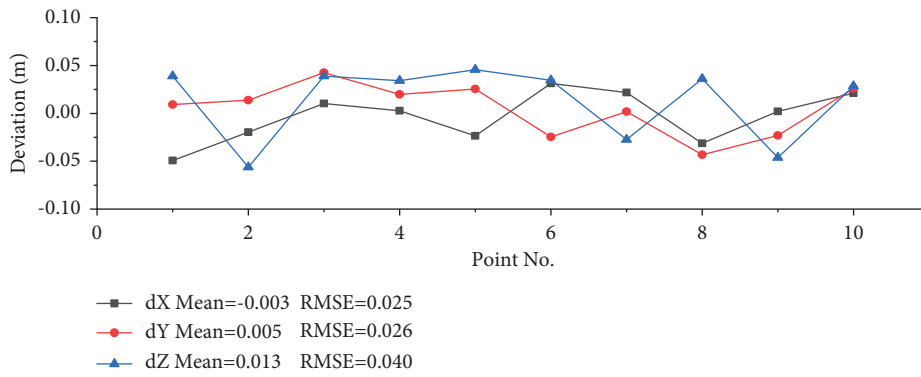


FIGURE 5: CPs deviation figure.

3.3. Spatial Feature Extraction

3.3.1. Spatial Feature Element Extraction. In the study, the spatial elements are divided into three types: water, architecture, and plants, and the spatial data of each type are extracted separately. Among them, water includes Tangan River and Xiaoxi Lake, architecture includes Shuikou buildings and ancestral temple, and plants include Shuikou trees and Shuikou forests.

In this paper, Acute3D Viewer was selected to extract the spatial data of elements in the 3D model. By using the measurement tool, the area, perimeter, and distance of the elements can be accurately calculated through the selection of the range. Therefore, the extraction can obtain the scope and morphological characteristics of the water, the structural characteristics of buildings, and the distribution characteristics of plants to meet the element spatial data extraction requirements.

3.3.2. Building and Street Space Extraction. In the filtering of point cloud, the CSF has high accuracy [32, 33]. In this paper, we take the point clouds on both sides of Tangan River as an example and use the modified CSF in CloudCompare software to extract the building surface. The overall process is as follows: set the cloth resolution, project the cloth particles, and point clouds horizontally. The point in the nearest point cloud of the cloth particles is found in the projection as the corresponding point of the particles. The point is denoted by P . The height before projection is HP , which is the lowest value that the cloth particle can descend to. The height of the particle in motion is denoted by H . After iteratively calculating H and H_p , if $H \leq H_p$, the particle is returned to the position of point P and the particle is set as immovable. The height difference between the points and particles in the point cloud is calculated, and if it is less than the set threshold H_{th} , it is a building point cloud, and vice versa it is a nonbuilding point cloud. The grid resolution in the test is 2 m, the maximum number of iterations is 500, and the threshold value is 0.5 m to get the extracted building point cloud (see Figure 6(b)). Finally, the shortest distance between all the roof point clouds in Figure 6(b) to their respective neighboring ground points in Figure 6(a) is calculated. The point cloud of the selected street elevation is segmented in the point cloud data, and the width of the street is calculated.

3.3.3. Terrain Extraction. DSM, as a new generation of digital mapping products, has the advantages of high accuracy, rich information, and detailed elevation information [34, 35]. In this study, DSM data were used as the basis for extracting terrain features of the Shuikou garden space. Slope and aspect analyses maps were obtained by using ArcGis 10.2 spatial analysis module. The DSM, slope, and aspect maps were combined to extract and analyze the terrain environmental features of Tangan. In addition, DSM contains surface elevation information other than ground level, and the obtained spatial analysis maps can also be used for the interpretation of building roof slope and aspect. This

method can extract terrain environment features on both sides of Tangan River in a more scientific and complete way, and the interpretation of the obtained analysis results will be more reliable.

4. Results

4.1. Orthophoto and 3D Model. After acquiring aerial images by oblique photography, UAVs combine specialized software and required steps to obtain accurate and complete 3D models and point cloud [36]. The produced results include orthophotos (see Figure 7) and DSM with centimeter-level accuracy, which are further used in the extraction and analysis work of spatial elements and terrain, such as calculation of volume and surface area of spatial elements, and slope and aspect analyses. This method of spatial feature extraction provides a richer form of data for traditional villages and helps researchers to carry out subsequent research and conservation work.

With the high-resolution aerial images acquired by UAV, accurate 3D models (see Figure 8) and point cloud can be obtained by using remote sensing and 3D reconstruction techniques. Among them, the higher the quality and quantity of the acquired images and the number of GCPs used, the better the overall quality of the model. The final results can quickly extract the spatial features of buildings, streets, and spatial elements. The geospatial and real-world information contained in the 3D model provide a complete record of the village spatial data from multiple perspectives, making up for the lack of text, photo, and video records.

The final orthophoto and 3D models provide scholars and local heritage conservation units with high-resolution data for development, conservation, and restoration studies of traditional villages. The accuracy and realism of the 3D models allow scholars from different places to understand the current status of the village heritage without traveling to the site, saving a lot of on-site investigation, and documentation work.

4.2. Spatial Feature Element

4.2.1. Water. As an important spatial feature element of Tangan, water body embodies the typical characteristics of Shuikou garden space. Through the extraction and analysis of water features in the 3D model, a result was obtained that water is not only the key to the creation of village geomancy but also an important component of the landscape system and the production and life of residents.

The measured effects in the 3D model show that Tangan River has an area of 3837.44 m² and a circumference of 1169.82 m, which crosses the whole village in space (see Figure 9(b)). From the perspective of the depth of the stream, the average depth of Tangan River on the west side of Goyang Bridge is 1.5 m, and on the east side is 2.5 m. This is due to the dam built under the bridge, which raises the upstream water level. The water flow has a very obvious drop at the gate of the dam, and the change of the drop solves the problem of water accumulation, and with the use of the gate it can well control the flow of water and serve the purpose of

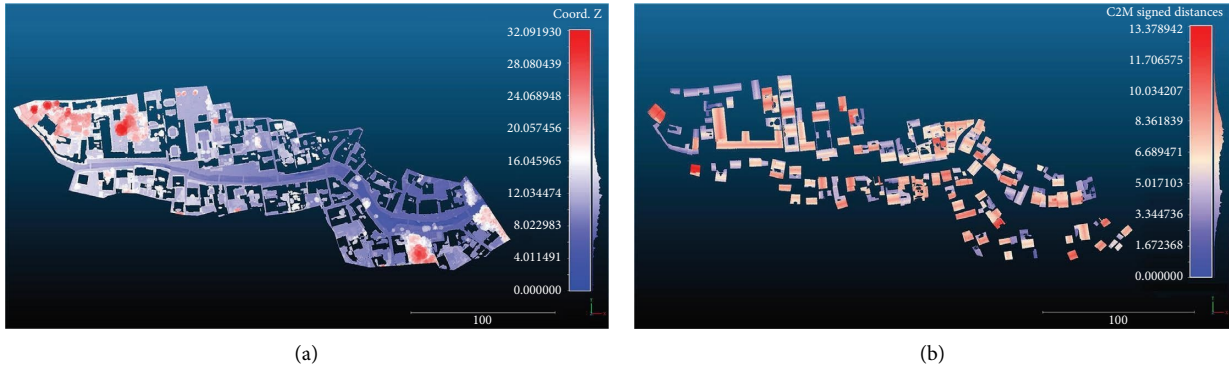


FIGURE 6: Point clouds on both sides of Tangan river. (a) Point clouds after removal of the building. (b) The building point cloud.

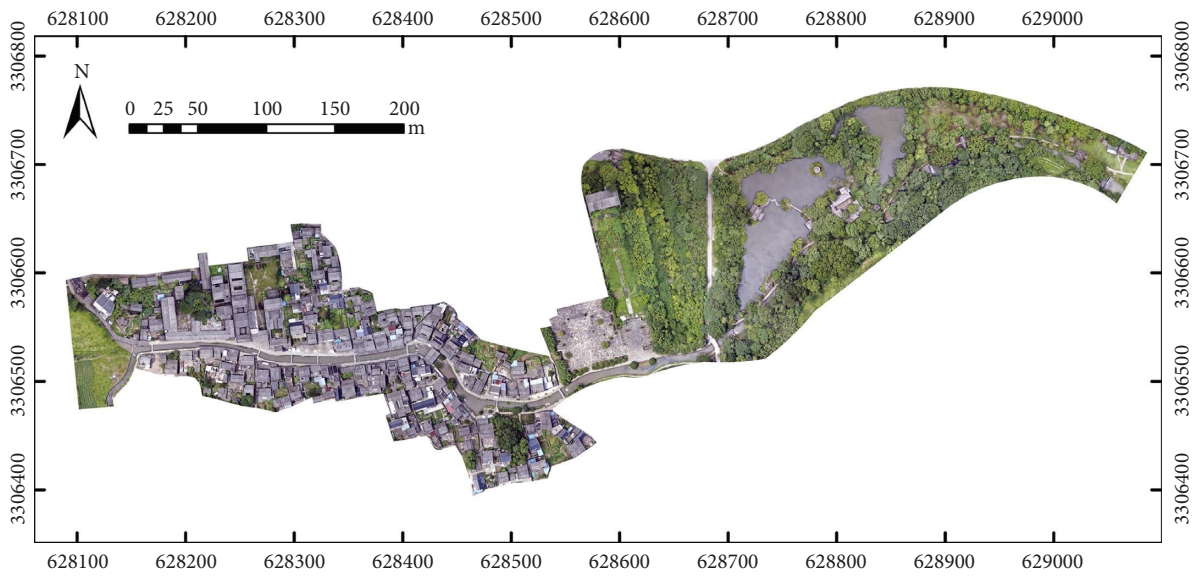


FIGURE 7: Obtained orthograph.

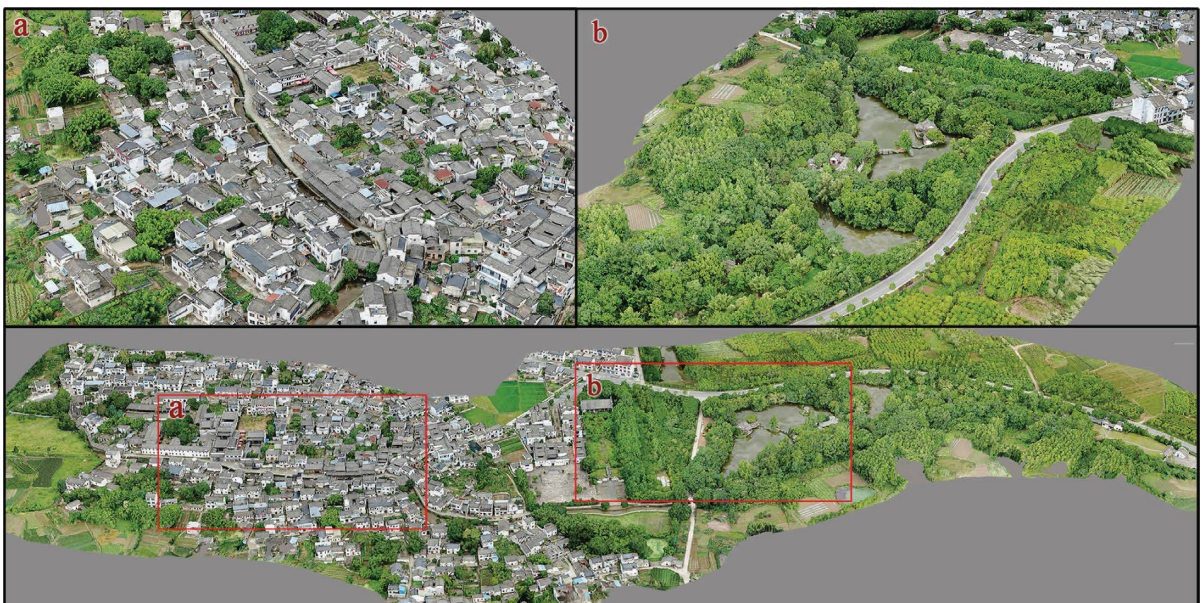


FIGURE 8: The photorealistic 3D model. (a) The aerial view of Tangan river. (b) Aerial view of Shuikou garden.



FIGURE 9: Water measurement in the 3D model. (a) Xiaoxi lake measurement. (b) Tangan river measurement.

water storage. The width of Tangan River is mainly between 4.5 m and 5.5 m. Among them, the width at the corner is between 7.8 m and 10.3 m, about twice the average width, which has the function of slowing down the water flow, reducing the impact of water, and ensuring the safety of the barge and the village. The small west lake on the east side has an area of 6246.80 m^2 and a perimeter of 430.52 m (see Figure 9(a)). Compared with the narrow Tangan River, the water surface of the small west lake is relatively open and wider in space.

4.2.2. Architecture. Tangmo Village has landscape elements such as pavilions, bridges, and memorial archway at the water outlets, playing the role of pointing and viewing, and becoming indispensable characteristic elements in the spatial organization of Shuikou garden. The style and dimensions of the buildings were extracted through the 3D realistic model, as in Table 2. The accuracy of the architectural data extraction directly affects the analysis results, so the manual measurement results were selected for the verification. From the comparative analysis of Tables 2 and 3, it can be seen that the errors of the length, width, and height of the buildings are within 5 cm, which meet the requirements of the extraction and analysis.

The memorial archway is spatially usually located at the opening part of the ancient building complex and is an identifying building on the space of the Shuikou garden. The memorial archway is 12.30 m high and only 2.5 m wide, and the plane is monogrammed, there is a large wind load. Therefore, stone lions and drum stones are placed on both sides of the stone columns of the memorial archway in the design. Among them, the stone lion and drum stones are 2.5 m high and 0.85 m wide, which play a good supporting and protecting role for the memorial archway. There are ten stone bridges in the village, among which Gao Yang Bridge is the most complex in design, consisting of pavilions and galleries. The bridge is 12.6 m long, 7.4 m wide, and 7.15 m high, meeting the needs of residents for passage and rest. The ancestral temple is the center of family politics, culture, rituals, and economy and is an indispensable part of the spatial element features. There are four ancestral temples in Tangmo Village, and for historical reasons, only Shang Yi Hall and Ji Shan Hall remain. Both halls are about 11 m in height and have a floor area of 690.75 m^2 and 502.00 m^2 ,

respectively, which are much larger in scale than the traditional buildings. Its role as a center of the ritual and communication for the inhabitants provides a spatial place of variety.

4.2.3. Plants. The creation of the plant landscape of Tangmo garden is unfolded in layers according to the changes of the Shuikou space. At the entrance of the Shuikou garden, there is a solitary ancient tree—camphor tree, which serves as the beginning of the spatial sequence of the Shuikou garden. According to the 3D model measurement (see Figure 10), the tree grows to a height of 31 m with a diameter of 3.6 m. After entering the water outlet, the trees on both sides of the Tangan River form a transitional space to Tangan Garden. Exotic flowers and plants are also planted around the pavilion, waterside pavilion, and other buildings in the garden to decorate the space. The 3D model shows that the plants are widely distributed around and inside the water outlet, and they are collectively called “Shuikou forest,” with a total area of $23,136.5 \text{ m}^2$. The dense planting of the Shuikou forest forms an ecological barrier in the environment, which plays the role of wind shelter, soil and water conservations, and microclimate regulation.

4.3. Terrain Feature. The analysis of surface elevation data represented by DSM shows the distribution range and surface elevation of the ground, buildings, and plants in the village space (see Figure 11). The surface elevation mainly ranges from 140 m to 143 m, showing a change in the elevation from high in the west to low in the east, which is consistent with the direction of the water flow of Tangan River flowing through the village. It indicates that the village follows the natural terrain changes in the construction and no major terrain modification works were carried out. In terms of the overall spatial distribution, the elevation of the west side is lower than the east side, which reduces the blocking effect on the southwest wind in summer and facilitates ventilation and temperature reduction. In addition, there is a 0.5 m–1 m drop from the outside of the village to the center so that the water converges is discharged through the Tangan River, effectively avoiding waterlogging. The top elevation of the plant is between 171 m and 145 m. Combined with the surface elevation data, it can be seen that the

TABLE 2: The extract building size and area from the 3D model.




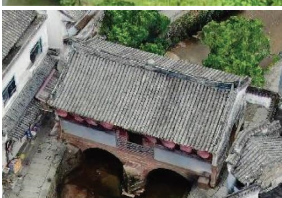

Architecture name	Architectural form	Length (m)	Width (m)	Height (m)	Area (m ²)
Shadi pavilion		6.43	6.46	12.22	41.54
Tongbao hanlin		9.95	2.55	12.33	34.19
Zimei pavilion		7.80	3.61	6.45	20.37
Gao Yang bridge		12.55	7.42	7.12	92.80
Shang Yi hall		44.96	15.35	10.91	690.14

TABLE 2: Continued.


Architecture name	Architectural form	Length (m)	Width (m)	Height (m)	Area (m ²)
Ji Shan hall		40.02	12.53	11.56	501.45

TABLE 3: The field measurement of the building size and area.

Architecture name	Length (m)	Width (m)	Height (m)	Area (m ²)
Shadi pavilion	6.45	6.45	12.26	41.60
Tongbao Hanlin	9.95	2.50	12.30	34.50
Zimei pavilion	7.85	3.60	6.43	20.55
Gao Yang bridge	12.60	7.40	7.15	93.24
Shang Yi hall	45.00	15.35	10.95	690.75
Ji Shan hall	40.00	12.55	11.55	502.00

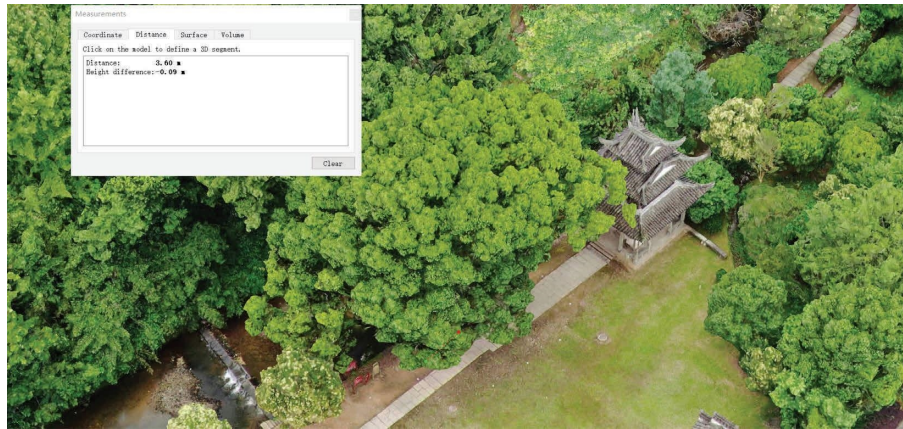


FIGURE 10: Camphor tree measurement.

plant height is between 5 m and 25 m, with a variety of canopy lines and abundant plant species.

From the perspective of the slope, the topography of Tangmo slopes between 0 degrees and 3 degrees (see Figure 12), and the terrain is flat, which is related to the location of the village in a flat area of the river valley. The flat topography ensures enough arable land for reclamation and basic production and living. At the same time, it is conducive to the construction of plazas and larger-scale buildings, providing a place for residents to interact with each other. Tangmo is located in the southern region of China, which has a subtropical monsoon climate with abundant precipitation in summer. Due to the natural environment, the roof slope of the buildings is large between 25 degrees and 30 degrees (see Figure 12), which is conducive to drainage.

The aspect is an important factor in the spatial features of villages. The aspect raster data extraction based on the digital surface model shows that the building roof aspect is in four directions south, north, east, and west, and the ground surface is mainly in three directions south, southwest, and west (see Figure 13), which leads to more light and heat available in winter to counteract the cold and wet winter climates. Adequate light meets the plants' growth requirements, and therefore village plants are planted with sunny species.

4.4. Spatial Features of the Building and Streets. The number of selected building point clouds changes with the building height as shown in Figure 14, where the number of point

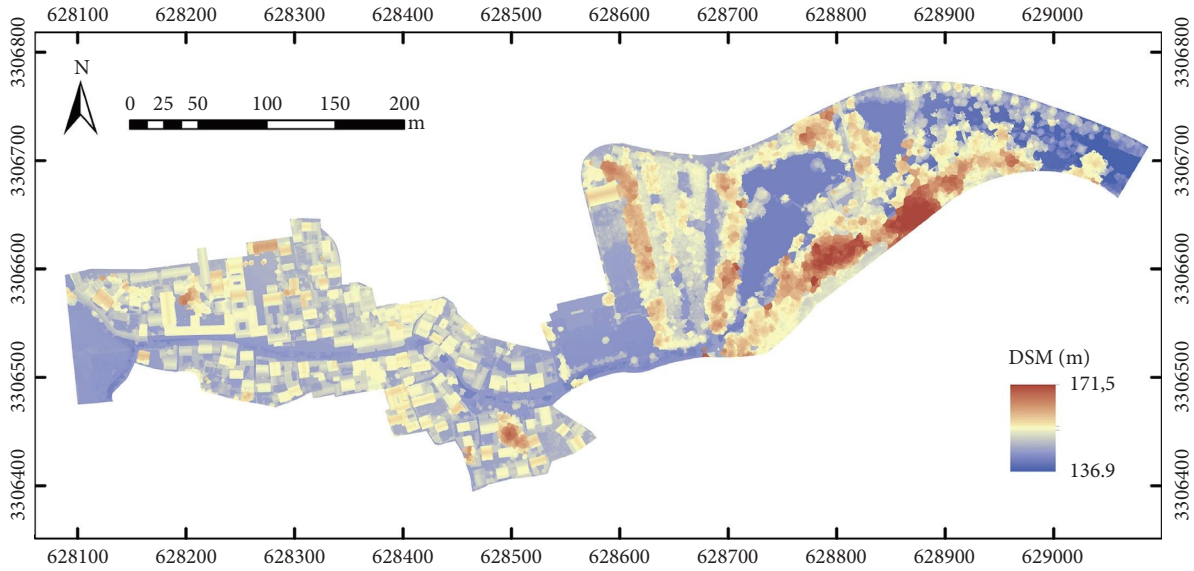


FIGURE 11: The digital surface area.

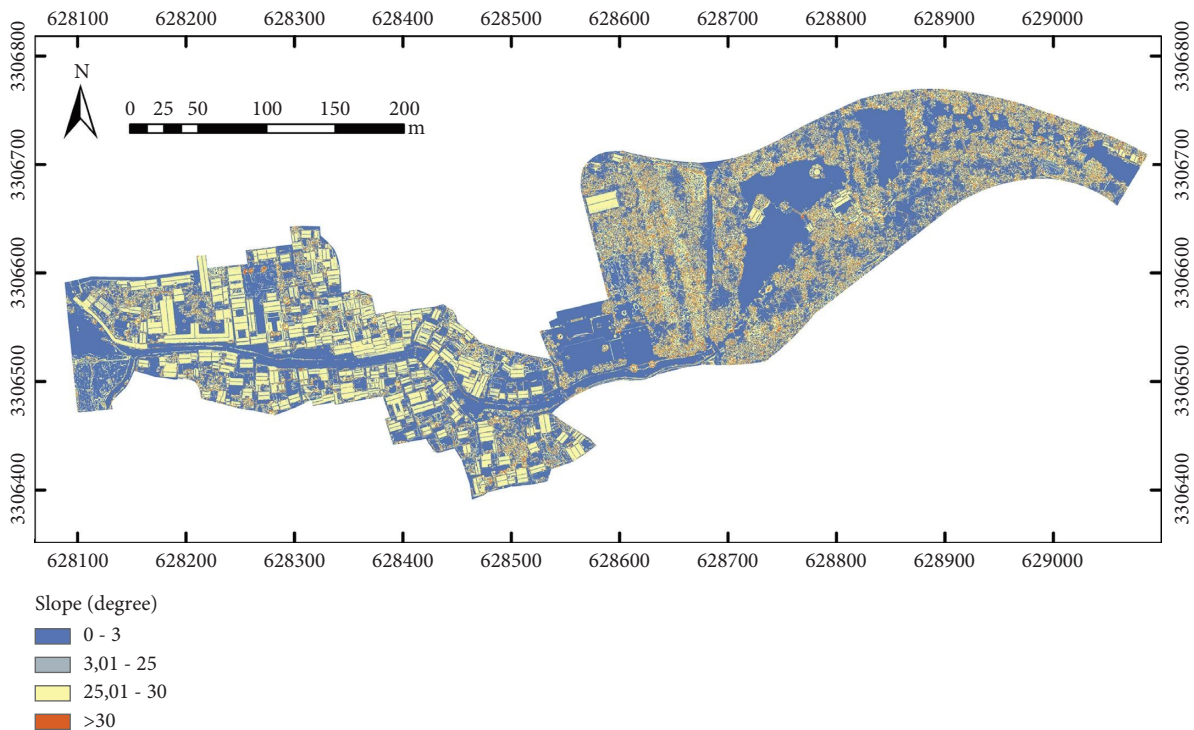


FIGURE 12: The slope illustration.

clouds in the height range of 7.2–8.3 m is the largest, followed by the number of point clouds in the height range of 4.2–4.8 m, and the number of point clouds in the two ranges show a precipitous decline at the heights of 8.3 m and 4.8 m, respectively. According to the decreasing trend of the two peaks presented in Figure 14, it is inferred that the buildings on both sides of Tangan River are mainly one-story buildings and two-story buildings, and the average

height is concentrated at 8.3 m–4.8 m, respectively. To verify the accuracy of the building height feature extraction method, the height statistics based on UAV and field measurements were performed for the selected 89 buildings with one-story and two-story buildings. The number of one-story and two-story buildings is 32 and 57 respectively, and the mean field measurement heights are 8.35 m–04.83 m respectively, with the fit degrees above 0.98

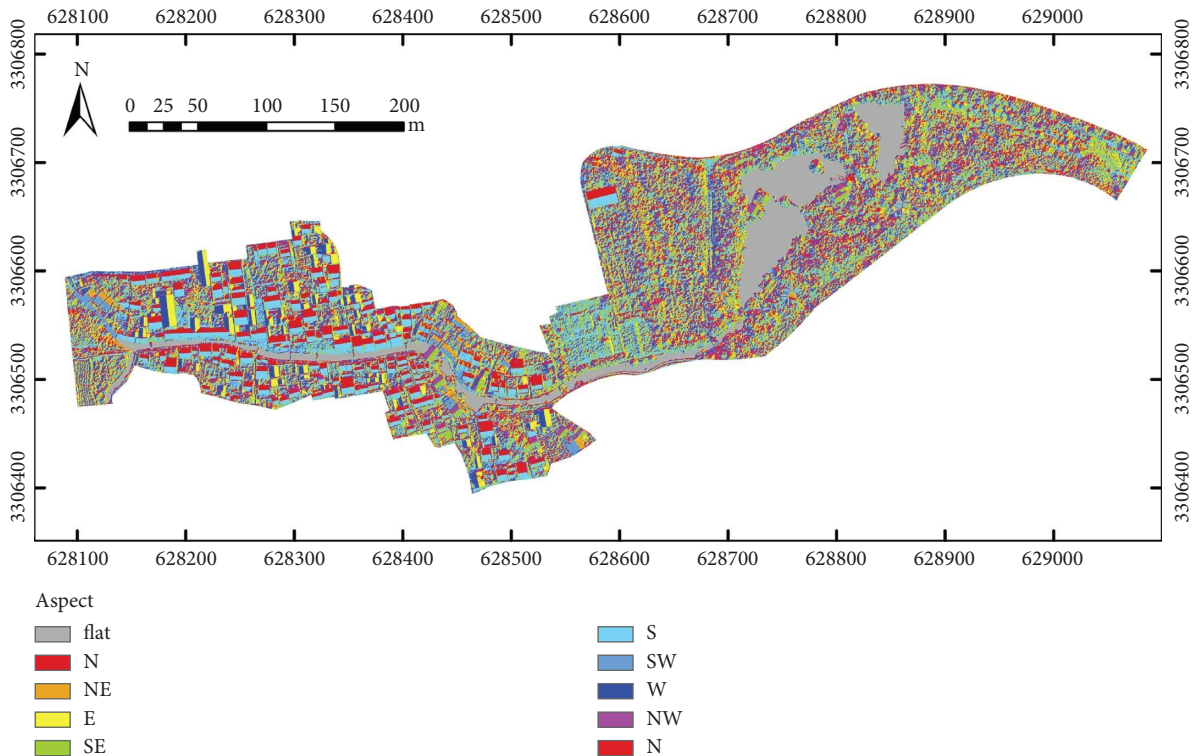


FIGURE 13: The aspect illustration.

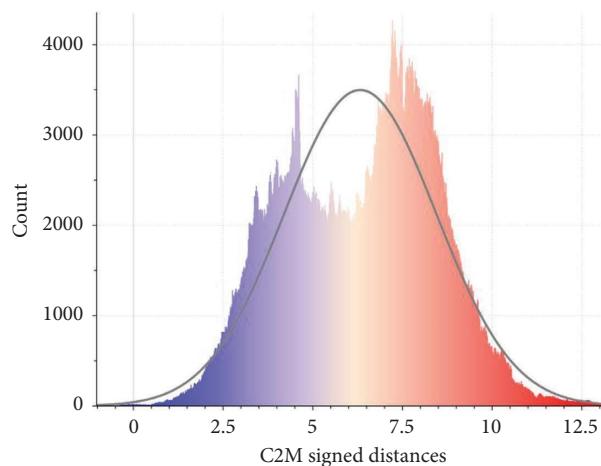


FIGURE 14: The roof point cloud height distribution from the ground. The horizontal axis is the height, and the vertical axis is the total number of point clouds at that height.

(see Figure 15). It proves that the method has high accuracy and can be used to quickly understand the spatial features of the buildings in a short time.

Figure 16 shows the street width variation map and the location map in the village selected in Tangmo. By analyzing the chart, we found that the width of the street space composed of buildings on both sides of the water street varies greatly, concentrating between 7.8–10.5 m and 12.8–14.2 m, much larger than the average width of the traditional village streets. This is because its role as the main

street provides the main traffic and residential activity place in the village. Comparing with other streets and alleys, we found that about 90% of the point cloud data are concentrated in the width range of 1–2.5 m. However, there is still a certain number of point clouds in the width range greater than 2.5 m. Combined with the field survey, we found that this part of the width was formed by the absence of the original building. For example, after the collapse of the original ancient residential building on the east side of Shang Yi Hall, the reconstructed building site was set back to the

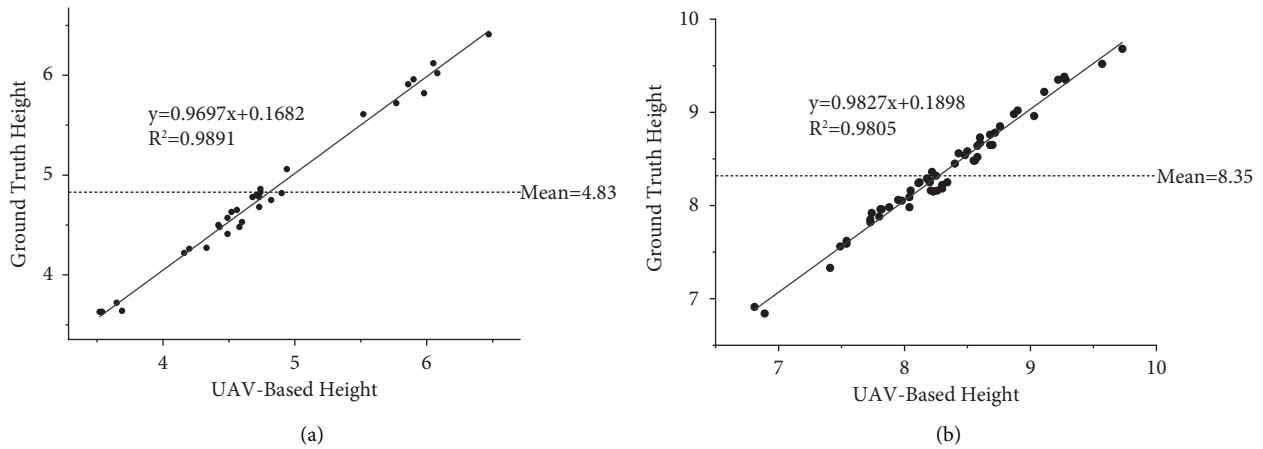


FIGURE 15: The correlation plot of the ground truth height and UAV-based height. (a) One-story correlation plots. (b) Two-story correlation plots.

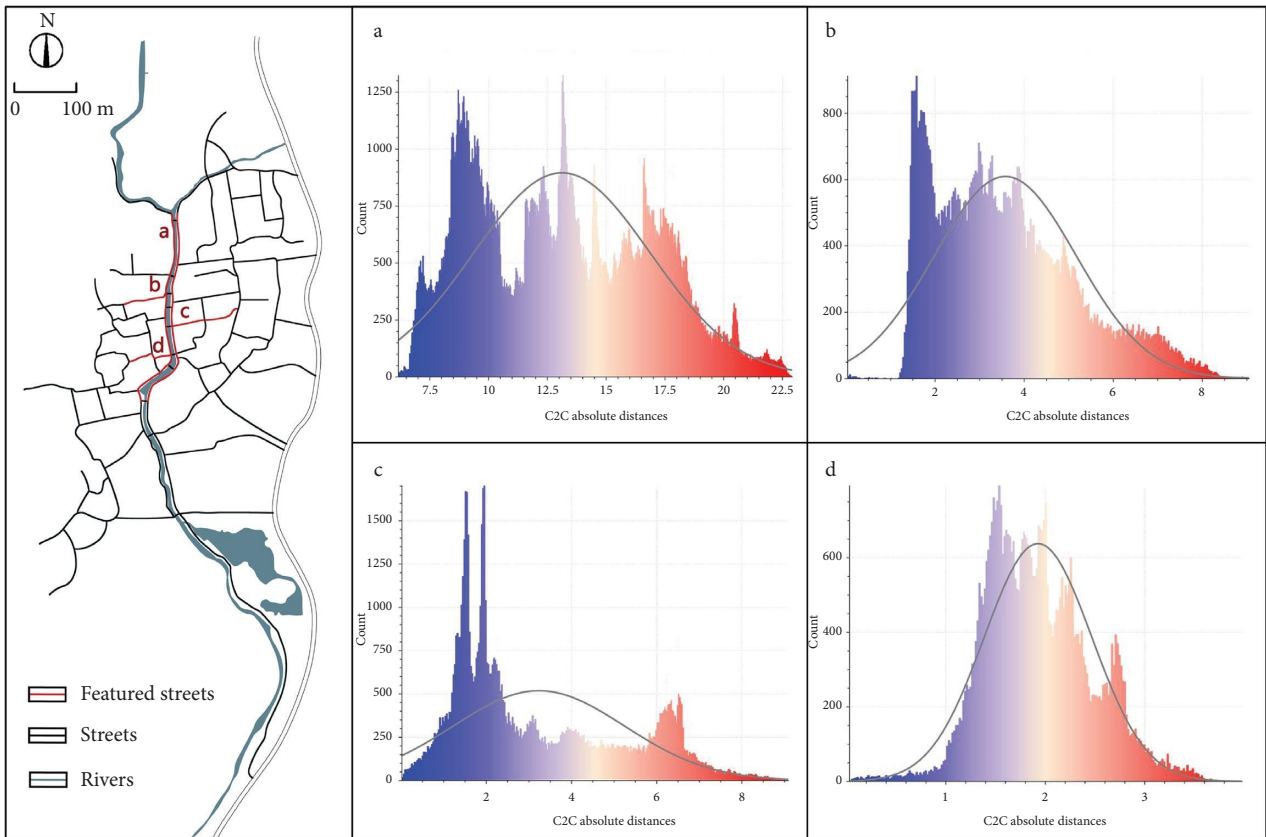


FIGURE 16: The range of street widths calculated for the selected characteristic streets. The horizontal axis is the street width, and the vertical axis is the total number of point clouds under this width.

north side, leading to the expansion of the original street space.

5. Discussion

5.1. Digital Conservation of Traditional Villages. The digital conservation and development of traditional villages need to collect multidimensional digital information. After

multilevel extraction and analysis and storage, it provides data support for the promotion of traditional villages and the repair of architectural sites, conservation research, and data development. Some scholars use multimedia technology to preserve traditional village data. However, this approach suffers from the problem of insufficient data richness. The 3D model products obtained from processing the UAV aerial images can clearly express the

basic information such as spatial forms, landscape elements, and architectural contours of villages. The spatial information of traditional villages is uploaded to the big data cloud computing platform for analysis and then stored in the corresponding database to build an integrated data service platform of Tangmo village, thus forming a virtual scene of village from multiple dimensions. The village database platform constituted by the efficient spatial data collection method of the UAV will accelerate the construction of a digital museum of traditional villages, provide virtualized interactive experiences for tourists, and further promote the development of village tourism and economy.

5.2. Providing Methodological Reference for Similar Studies. With rapid urban development and modernization, more and more traditional villages are changing under the influence of various factors, resulting in the extinction of characteristic spatial features inherited for thousands of years [37–39]. Therefore, it is hoped that more scholars will conduct research related to the spatial conservation of traditional villages and conduct in-depth studies on how these spatial data can be collected and extracted. This paper provides a research methodology from data collection to spatial feature extraction. Firstly, aerial images of traditional villages are acquired through suitable flight plans. Secondly, 3D models, DOM, and DSM data are produced by using Context Capture software, and the accuracy of the produced data is corrected and checked by obtaining GCPs using handheld RTK. Then, the spatial features of traditional villages are extracted from the produced data by analysis software. Finally, the impact of the spatial morphological features on the production and life of the residents is analyzed based on the extraction results. This method of spatial data collection and feature extraction can be applied to other traditional village studies and has wide applicability and application value, providing more accurate and richer spatial data for the study of traditional villages.

5.3. Shortcomings and Outlook. Although the use of UAV for spatial data collection is the more advanced of the current data collection means, there are technical limitations. For example, mapping data cannot be obtained for mapping targets that are obscured by trees or shrubs, etc., due to the low height of traditional buildings. In the future, in traditional village spatial data collection, UAV data collection can be organically combined and integrated with 3D laser scanning technology. Combining ground and air data, data collection can be carried out from multiple angles to further improve data accuracy and collection efficiency. In order to analyze and evaluate the specific spatial data needs, measurement technology, and data processing, we will consider the data accuracy, expression effect, processing efficiency, and other factors and choose one or more suitable technologies to carry out the actual data collection work.

6. Conclusion

This paper takes Tangmo as the research object, exploring a method to acquire spatial data of villages based on UAV aerial images and extract spatial feature information from them. At the same time, it provides new ideas and methods for studying the extraction and analysis of spatial feature data of traditional villages. In addition, the extracted spatial feature data have a practical significance for the research, development, and conservation of Tangmo. The specific conclusions are as follows:

- (1) The use of UAV aerial imagery combined with the GCPs measured in the field ensures the accuracy requirements of the photogrammetric products. By checking the accuracy of the spatial data, the RMSE is 0.034 m horizontally and 0.039 m vertically. It is proved that the data acquisition method of this paper is suitable for the collection of spatial data of traditional villages, and it is more efficient and accurate.
- (2) The 3D model can completely record and extract the characteristic data of water, building, and plant spatial elements. The extraction of village terrain feature data is realized with the help of spatial data consisting of digital surface model (DSM) and slope and aspect data. The spatial features of streets and buildings were extracted through segmentation processing and fast statistical extraction of the selected street point cloud. Based on the analysis of the extraction results, it is concluded that the spatial layout of Tangmo follows the natural environment, and the buildings are built along the stream to meet the needs of residents' production and living and ecological environments, which is consistent with the spatial features of Shuikou garden.
- (3) The DOM, DSM, and 3D model of Tangmo can provide scholars with virtual scenes possessing real feelings and complete records of all kinds of spatial information. Combined with the extracted spatial feature data can be used to establish a complete village database after the classification and storage, which provide data basis for the research, protection, restoration, and innovative development of traditional villages.

Data Availability

The data used to support the findings of this study are available from the corresponding author upon request.

Conflicts of Interest

The authors declare that they have no conflicts of interest regarding the publication of this paper.

Acknowledgments

This research was funded by the National Key R&D Program of China (Funding number: 2017YFC0505706) and

University Natural Science Research Project of Anhui Province (Funding number: KJ2021A0161).

Supplementary Materials

Table S1 is the UAV-SfM model accuracy assessment GCPs. Table S2 is the UAV-SfM model accuracy assessment CPs. (*Supplementary Materials*)

References

- [1] J. Bian, W. Chen, and J. Zeng, "Spatial distribution characteristics and influencing factors of traditional villages in China," *International Journal of Environmental Research and Public Health*, vol. 19, no. 8, Article ID 19084627, 2022.
- [2] Z. Y. Cai, J. Li, and J. Wang, "The protection and landscape characteristics of traditional villages in coastal areas of SW China," *Journal of Coastal Research*, vol. 111, no. 1, pp. 331–335, 2020.
- [3] J. Xu, M. S. Yang, C. P. Hou, Z. L. Lu, and D. Liu, "Distribution of rural tourism development in geographical space: a case study of 323 traditional villages in Shaanxi, China," *European Journal of Remote Sensing*, vol. 54, no. 2, pp. 318–333, 2021.
- [4] J. J. Zhou, C. Hua, S. S. Wu, Z. R. Wang, and X. K. Wang, "Sustainable village planning indicator system in rural transformation: application to xufu village in the yangtze river delta region in China," *Journal of Urban Planning and Development*, vol. 147, no. 4, p. 147, 2021.
- [5] Y. Sun and Q. F. Ou, "Research on the traditional zoning, evolution, and integrated conservation of village cultural landscapes based on "production-living-ecology spaces" - a case study of villages in Meicheng, Guangdong, China," *Open Geosciences*, vol. 13, no. 1, pp. 1303–1317, 2021.
- [6] R. J. Qin and H. H. Leung, "Becoming a traditional village: heritage protection and livelihood transformation of a Chinese village," *Sustainability*, vol. 13, no. 4, Article ID 13042331, 2021.
- [7] H. Ma and Y. Tong, "Spatial differentiation of traditional villages using ArcGIS and GeoDa: a case study of Southwest China," *Ecological Informatics*, vol. 68, Article ID 101416, 2022.
- [8] S. Liu, J. Ge, W. M. Li, and M. Bai, "Historic environmental vulnerability evaluation of traditional villages under geological hazards and influencing factors of adaptive capacity: a district-level analysis of lishui, China," *Sustainability*, vol. 12, no. 6, Article ID 12062223, 2020.
- [9] Q. Zhang, Y. Liu, L. Liu, S. Lu, and J. Zhang, "Strategy analysis for the interaction between tourism development and local eco-environment in traditional villages," *Journal of Environmental Protection and Ecology*, vol. 21, pp. 2279–2289, 2020.
- [10] L. Xu and S. C. Chiou, "A study on the public landscape order of xinye village," *Sustainability*, vol. 11, no. 3, Article ID 11030586, 2019.
- [11] J. Fu, J. Zhou, and Y. Deng, "Heritage values of ancient vernacular residences in traditional villages in Western Hunan, China: spatial patterns and influencing factors," *Building and Environment*, vol. 188, Article ID 107473, 2021.
- [12] X. Yang, K. Song, and F. Pu, "Laws and trends of the evolution of traditional villages in plane pattern," *Sustainability*, vol. 12, no. 7, Article ID 12073005, 2020.
- [13] G. Lin, A. Giordano, K. Sang, L. Stendardo, and X. Yang, "Application of territorial laser scanning in 3D modeling of traditional village: a case study of Fenghuang village in China," *ISPRS International Journal of Geo-Information*, vol. 10, no. 11, Article ID 10110770, 2021.
- [14] J. Shao, W. Zhang, N. Mellado et al., "Automated markerless registration of point clouds from TLS and structured light scanner for heritage documentation," *Journal of Cultural Heritage*, vol. 35, pp. 16–24, 2019.
- [15] A. Kyriou, K. Nikolakopoulos, and I. Koukouvelas, "How image acquisition geometry of UAV campaigns affects the derived products and their accuracy in areas with complex geomorphology," *ISPRS International Journal of Geo-Information*, vol. 10, no. 6, p. 408, 2021.
- [16] S. Y. Guan, Z. Zhu, and G. Wang, "A review on UAV-based remote sensing technologies for construction and civil applications," *Drones*, vol. 6, no. 5, Article ID 6050117, 2022.
- [17] L. S. Grigore, A. G. Stefan, O. Orban, and I. R. Adochiei, "Considerations on the plastic structure of a UAV payload made by 3D printing technology," *Materiale Plastice*, vol. 57, no. 4, pp. 21–33, 2021.
- [18] S. Biçici and M. Zeybek, "Effectiveness of training sample and features for random forest on road extraction from unmanned aerial vehicle-based point cloud," *Transportation Research Record: Journal of the Transportation Research Board*, vol. 2675, no. 12, pp. 401–418, 2021.
- [19] Y. L. Yeh, "The standard strength test of 3D printing materials and its application for UAV propellers," *Modern Physics Letters B*, vol. 34, no. 9, Article ID 2040017, 2020.
- [20] W. Budiharto, E. Irwansyah, J. S. Suroso, A. Chowanda, H. Ngarianto, and A. A. S. Gunawan, "Mapping and 3D modelling using quadrotor drone and GIS software," *Journal of Big Data*, vol. 8, no. 1, p. 48, 2021.
- [21] M. Schaefer, R. Teeuw, S. Day et al., "Low-cost UAV surveys of hurricane damage in Dominica: automated processing with co-registration of pre-hurricane imagery for change analysis," *Natural Hazards*, vol. 101, no. 3, pp. 755–784, 2020.
- [22] A. Kyriou, K. G. Nikolakopoulos, and I. K. Koukouvelas, "Timely and low-cost remote sensing practices for the assessment of landslide activity in the service of hazard management," *Remote Sensing*, vol. 14, no. 19, Article ID 14194745, 2022.
- [23] M. Soroush, A. Mehrtash, E. Khazraee, and J. A. Ur, "Deep learning in archaeological remote sensing: automated qanat detection in the kurdistan region of Iraq," *Remote Sensing*, vol. 12, no. 3, Article ID 12030500, 2020.
- [24] K. G. Nikolakopoulos, K. Soura, I. K. Koukouvelas, and N. G. Argyropoulos, "UAV vs classical aerial photogrammetry for archaeological studies," *Journal of Archaeological Science: Report*, vol. 14, pp. 758–773, 2017.
- [25] P. Sestras, S. Roşca, Ş. Bilaşco et al., "Feasibility assessments using unmanned aerial vehicle technology in heritage buildings: rehabilitation-restoration, spatial analysis and tourism potential analysis," *Sensors*, vol. 20, no. 7, Article ID 20072054, 2020.
- [26] H. Hidayat and B. Muljo Sukojo, "Analysis of horizontal accuracy for large scale rural mapping using rotary wing UAV image," *IOP Conference Series: Earth and Environmental Science*, vol. 98, Article ID 012052, 2017.
- [27] D. Wang and D. Z. Li, "The cognition of the spatial art forms of tourist villages based on ecological engineering and sustainable development," *Ecological Chemistry and Engineering S*, vol. 28, no. 4, pp. 581–595, 2021.
- [28] J. L. Li, J. L. Chu, Y. Z. Wang, M. Ma, and X. G. Yang, "Reconstruction of traditional village spatial texture based on

- parametric analysis,” *Wireless Communications and Mobile Computing*, vol. 2022, Article ID 5151421, 21 pages, 2022.
- [29] I. Elkhachy, “Accuracy assessment of low-cost unmanned aerial vehicle (UAV) photogrammetry,” *Alexandria Engineering Journal*, vol. 60, no. 6, pp. 5579–5590, 2021.
- [30] Y. Taddia, L. Gonzalez-Garcia, E. Zambello, and A. Pellegrinelli, “Quality assessment of photogrammetric models for facade and building reconstruction using DJI phantom 4 RTK,” *Remote Sensing*, vol. 12, no. 19, Article ID 12193144, 2020.
- [31] M. Zeybek, “Accuracy assessment of direct georeferencing UAV images with onboard global navigation satellite system and comparison of CORS/RTK surveying methods,” *Measurement Science and Technology*, vol. 32, no. 6, Article ID 065402, 2021.
- [32] M. Zeybek and İ Şanlıoğlu, “Point cloud filtering on UAV based point cloud,” *Measurement*, vol. 133, pp. 99–111, 2019.
- [33] M. Zeybek, “Classification of uav point clouds by random forest machine learning algorithm,” *Turkish Journal of Engineering*, vol. 5, no. 2, pp. 51–61, 2021.
- [34] R. Bi, S. Gan, X. P. Yuan et al., “Studies on three-dimensional (3D) accuracy optimization and repeatability of UAV in complex pit-rim landforms as assisted by oblique imaging and RTK positioning,” *Sensors*, vol. 21, no. 23, Article ID 21238109, 2021.
- [35] M. Ebrahimikia and A. Hosseininaveh, “True orthophoto generation based on unmanned aerial vehicle images using reconstructed edge points,” *Photogrammetric Record*, vol. 37, no. 178, pp. 161–184, 2022.
- [36] S. Biçici and M. Zeybek, “An approach for the automated extraction of road surface distress from a UAV-derived point cloud,” *Automation in Construction*, vol. 122, Article ID 103475, 2021.
- [37] L. K. Lin, C. L. Du, Y. Yao, and Y. Gui, “Dynamic influencing mechanism of traditional settlements experiencing urbanization: a case study of Chengzi Village,” *Journal of Cleaner Production*, vol. 320, Article ID 128462, 2021.
- [38] Y. Liu, L. Liu, S. Lu, and Q. Zhang, “Ecological landscape resource management and sustainable development of traditional villages,” *Journal of Environmental Protection and Ecology*, vol. 21, pp. 1938–1949, 2020.
- [39] L. Feng, B. Chen, T. Hayat, A. Alsaedi, and B. Ahmad, “The driving force of water footprint under the rapid urbanization process: a structural decomposition analysis for Zhangye city in China,” *Journal of Cleaner Production*, vol. 163, pp. S322–S328, 2017.